Journal of Luminescence 131 (2011) 2144–2147

Contents lists available at ScienceDirect

Journal of Luminescence

journal homepage: www.elsevier.com/locate/jlumin

# Efficient white organic light-emitting diodes based on an orange iridium phosphorescent complex

Ping Chen [a,*], Li Zhao [a], Yu Duan [a], Yi Zhao [a], Wenfa Xie [a], Guohua Xie [a], Shiyong Liu [a,*], Liying Zhang [b], Bin Li [b]

[a] State Key Laboratory on Integrated Optoelectronics, College of Electronic Science and Engineering, Jilin University, Changchun 130012, People's Republic of China
[b] Key Laboratory of Excited State Processes, Changchun Institute of Optics, Fine Mechanics and Physics, Chinese Academy of Sciences, Changchun 130033, People's Republic of China

ARTICLE INFO

*Article history:*
Received 15 February 2011
Received in revised form
5 May 2011
Accepted 16 May 2011
Available online 26 May 2011

*Keywords:*
Blue fluorescence
Orange phosphorescence
White
OLED

ABSTRACT

Stable and efficient white light emission is obtained by mixing blue fluorescence and orange phosphorescence. The introduction of double exciton blocking layers brings about well confinement of both charge-carriers and excitons in the emission layer. By systematically adjusting blue fluorescent and orange phosphorescent emission layers thickness, carriers in emission zone are balanced, and electrically generated excitons can be efficiently utilized. One white device with power efficiency of 14.4 lm/W at 100 cd/m$^2$ has excellently stable spectra. The improvement of performance is attributed to efficient utilization of the excitons and more balance of charge-carriers in emission layer.



## 1. Introduction

White organic light-emitting devices (WOLEDs) have attracted a lot of attention recently for their potential use in full-color flat-panel display, as solid state lighting sources or back light for liquid crystal display [1–5]. Because phosphorescent materials have a potential for achieving 100% internal quantum efficiency due to the ability of harvesting both singlet and triplet excitons [6], WOLEDs based on all phosphorescent materials show higher efficiency. But the use of wide band-gap host materials for blue phosphorescent dyes will cause high turn-on voltage, which affects the improvement of power efficiency [4]. Though WOLEDs based on fluorescent materials have lower turn-on voltage and longer lifetimes, the efficiency is limited by only using singlet excitons to emit fluorescence [7]. In order to solve the conflict, the concept that uses a fluorescent dye to harvest singlet excitons for blue fluorescent emission and the remainder of triplet excitons for green and red phosphorescent emission can reach a 100% internal quantum efficiency and higher power efficiency [3,5,8–11].

White light emission can be obtained by mixing three primary colors [3–5,12–14] or two complementary colors [11,15–19]. Compared with WOLEDs based on three primary colors, WOLEDs based on complementary colors have simple structures and stable spectra, but the efficiency is much lower. Moreover, there are few reports about WOLEDs based on two complementary colors to utilize all generated excitons [11,19]. Recently, Bhansali et al. [19] demonstrated WOLEDs based on yellow phosphor of Pt(II) complex and blue fluorescent material. The optimized WOLED exhibits good stability of color with power efficiency of 6 lm/W.

In this letter, we demonstrate more efficient WOLEDs based on blue fluorescent and orange phosphorescent materials. By introducing double exciton blocking layer and adjusting blue and orange emission thickness, charge-carriers and excitons are confined well in emission layer. One white device has power efficiencies of 14.4 and 10.1 lm/W obtained at 100 and 1000 cd/m$^2$, respectively, which is two times as high as that of the similar device [18]. Moreover, it also shows excellently stable spectra over a wide range of luminance.

## 2. Experiment

Clean glass coated by Indium Tin oxide (ITO) is used as transparent anode. 4,4′,4″-tris(3-methylphenylphenylamino)-triphenylamine (m-MTDATA) and N,N′-bis-(1-naphthyl)-N,N′-diphenyl-1,1′-biphenyl-4,4′-diamine (NPB) are used as hole-injection layer and hole-transportation layer, respectively. *fac*-tris(1-phenypyrazolyl-*N*,*C*2′)iridium(III) [Ir(ppz)$_3$] is used as electron and exction blocking layer. A common host material 4,4′-N,N′-dicarbazole-biphenyl (CBP) doped with 4,4′-bis(9-ethyl-3-carbazovinylene)-1,1′-biphenyl (BCzVBi) and bis(2-(2-fluorphenyl)-1,3-benzothiozolato-N,C2′)iridium(acetylacetonate) [(F-BT)$_2$Ir(acac)] are used as blue fluorescent emission and orange phosphorescent emission layer, respectively. 4,7-diphenyl-1,10-phenanthroline (Bphen) and tris (8-quinolinolato)aluminum (III) (Alq$_3$) act as hole blocking layer

* Corresponding authors.
*E-mail addresses:* chenping0329@gmail.com (P. Chen), syliu@jlu.edu.cn (S. Liu).

0022-2313/$ - see front matter © 2011 Elsevier B.V. All rights reserved.
doi:10.1016/j.jlumin.2011.05.038

and electron-transporting layer. Finally, 0.8 nm LiF covered by 100 nm Al is used as cathode. $(F\text{-}BT)_2Ir(acac)$ was synthesized and sublimated by ourselves, which can obtain high efficiency over a wide range of current densities, and the highest occupied molecular orbital (HOMO) and the lowest unoccupied molecular orbital (LUMO) energy levels of (F-BT)Ir(acac) are 3.4 and 5.8 ev, respectively [20]. Other materials were purchased from company. All organic layers were grown in succession by high vacuum ($3\times10^{-4}$ Pa) thermal evaporation at a rate of 0.1–0.2 nm/s. The layer thickness and the deposition rate of materials were monitored in situ by an oscillating quartz thickness monitor. EL spectra and Commission International de L'Eclairage (CIE) coordinates of the devices were measured using a PR650 spectroscan spectrometer. The luminance–voltage and current–voltage characteristics were measured simultaneously with the measurement of the EL spectra by combining the spectrometer with a programmable Keithley 2400 voltage–current source. All measurements were carried out at room temperature under ambient conditions.

## 3. Results and discussion

In order to determine the thickness of blue fluorescent layers to utilize all generated singlet excitons, we fabricated four blue devices with the following structure: ITO/m-MTDATA (30 nm)/NPB (10 nm)/$Ir(ppz)_3$ (10 nm)/CBP: 5 wt% BCzVBi (X nm)/CBP [(30-2X) nm]/CBP: 5 wt% BCzVBi (X nm)/Bphen (20 nm)/$Alq_3$ (20 nm)/LiF (0.8 nm)/Al (100 nm). For device A, $X=2$ nm; device B, $X=5$ nm; device C, $X=10$ nm; and device D, $X=15$ nm. Fig. 1 shows the structure and the energy level diagram. The thickness of emission zone is kept at 30 nm for the four devices. From the energy level diagram, we can tell charge recombination zones mainly locate at the $Ir(ppz)_3$/CBP and CBP/Bphen interfaces due to the fact that large densities of holes and electrons pile up at the energy barriers at the two interfaces. So blue fluorescent layers are placed at edges of emission zone to harvest short-diffusion length singlet excitons.

Fig. 2 shows the non-normalized electroluminescent (EL) spectra of the four blue devices A–D at the same current density of 10 mA/cm$^2$. The spectra show only one emission peak at 445 nm with a shoulder at 472 nm, which is originated from BCzVBi. The absence of CBP emission indicates that the energy transfer to BCzVBi is very efficient. When the thickness of blue emission layers is only 2 nm, the emission intensity is weakest because the recombination zone could be outside the blue emitting layer, which wastes some exictons. The intensity increases sharply with the increase in the thickness from 2 to 5 nm. But when it gradually increases from 5 to 15 nm, it shows almost no change. Table 1 summarizes the performances of the devices A–D. The maximum efficiency of device A is only 1.77 cd/A, while that of device B is 3.01 cd/A, which is almost the same as devices C and D. The luminance of device B is 6693 cd/m$^2$ at 11 V. We think the optimized thickness of the blue fluorescent layer at both interfaces of emission zone to utilize generated singlet excitons is 5 nm.

Efficient WOLEDs are demonstrated by fixing the thickness of blue fluorescent layers at 5 nm and inserting orange phosphorescent layer in the middle of blue emission layers to harvest triplet exictons whose diffusion length on CBP is about 40 nm [3]. Fig. 3 shows the structure and the energy level diagram of WOLEDs. The structure of WOLEDs is: ITO/m-MTDATA (30 nm)/NPB (10 nm)/$Ir(ppz)_3$ (10 nm)/CBP: 5 wt% BCzVBi (5 nm)/CBP (Y nm)/CBP: 8 wt% $(F\text{-}BT)_2Ir(acac)$ (Z nm)/CBP (Y nm)/CBP: 5 wt% BCzVBi (5 nm)/Bphen (20 nm)/$Alq_3$ (20 nm)/LiF (0.8 nm)/Al (100 nm). For device E: $Y=0$, $Z=5$ nm; device F: $Y=3$ nm, $Z=5$ nm; device G: $Y=3$ nm, $Z=10$ nm; device H: $Y=3$ nm, $Z=15$ nm. 3 nm neat CBP layer is introduced in devices F, G, H between blue and orange emission layers to suppress singlet energy transfer. The thickness of orange phosphorescent layer is adjusted to efficiently harvest triplet excitons. Fig. 4 shows normalized EL spectra of the four devices E–H at the current

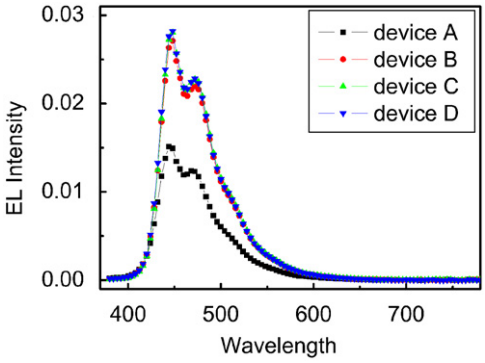


**Fig. 2.** Non-normalized EL spectra of the devices A–D at the current density of 10 mA/cm$^2$.

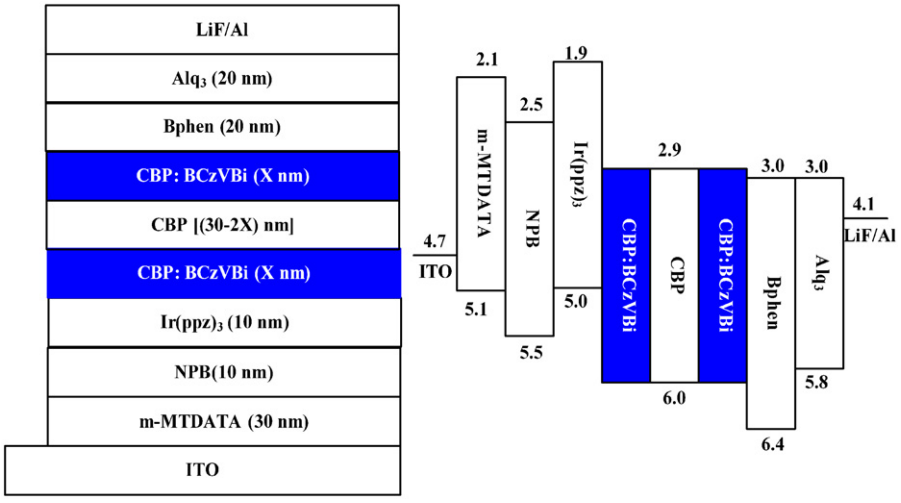


**Fig. 1.** Structure and the energy level diagram of blue devices A–D. For device A, $X=2$ nm; device B, $X=5$ nm; device C, $X=10$ nm; and device D, $X=15$ nm.

density of 10 mA/cm$^2$. All the spectra of the devices show two primary peaks originating from BCzVBi and (F-BT)$_2$Ir(acac). The strong emission intensity of (F-BT)$_2$Ir(acac) mainly comes from triplet excitons that have diffused through CBP from both emission layer interfaces, a small fraction comes from charge trapping that excitons formation on (F-BT)$_2$Ir(acac). When we introduce 3 nm neat CBP layer between blue fluorescent and phosphorescent emission layers, the intensity of blue emission increases relative to that of orange emission due to the fact that the energy transfer from singlet excitons on BCzVBi to lower energy (F-BT)$_2$Ir(acac) was prevented by the neat CBP layer. Both the blue and orange emission intensity increases when the thickness of orange emission layer increases from 5 to 10 nm, and then decreases with the increase in thickness to 15 nm. As known to all, exciton blocking layer Bphen and Ir(ppz)$_3$ can well confine excitons in emission layer due to their wider energy gap than those of host and dopant materials. But when the emission zone is very thin (for devices E and F), some charge-carriers can diffuse into blocking layers and recombine non-radiatively, which causes the charge-carriers imbalance in emission layer and the weaker emission intensity. When the emission zone is too wide (for device H), the density of charge-carriers in emission layer is reduced, as well as the exciton formation probability. Performances of the WOLEDs E–H are summarized in Table 2. All the devices emit warm white light and device G has a highest power efficiency of 14.8 lm/W with CIE coordinates of (0.383, 0.418). The color rendering index (CRI) of device G is only 60, which is very low according to the literature [22], it's because our device utilizes only two complementary colors to obtain white light emission. Moreover, the turn-on voltage of device G is 3 V and the maximum luminance is 40,870 cd/m$^2$ obtained at 13 V, which can be seen in Fig. 5.

Fig. 6 shows the normalized EL spectra of the white device G at different luminance from 5 to 19,810 cd/m$^2$. The spectra are very stable especially at higher luminance. It's because the ratio of singlets to triplets is always constant (1:3), as well as the relative intensity of blue–orange. Moreover, the triplet lifetime of (F-BT)$_2$Ir(acac) is very short [20], so the quenching effects of triplet–triplet annihilation is negligible, which is also good to the stable spectra at high luminance. The relatively higher emission intensity of orange light at 5 cd/m$^2$ is attributed to charge-trapping effect of (F-BT)$_2$Ir(acac), which is more severe in low current density [21]. Fig. 7 shows the power efficiency–luminance characteristics of device G. The power efficiency at 100 and 1000 cd/m$^2$ are 14.4 and 10.1 lm/W, respectively. The efficiency is much higher than the device with similar materials, which has efficiency less than 7 lm/W [18]. Note that if more efficient materials are adopted in combination with electrically doped transport layers, the performance can be further improved.

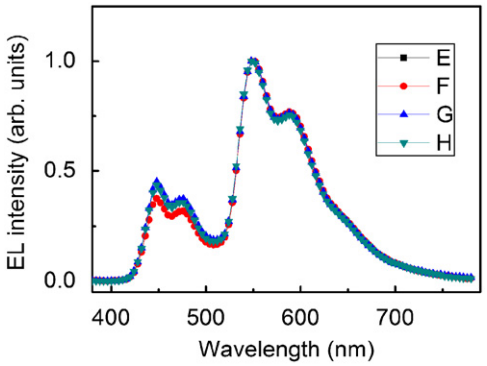


**Fig. 4.** Normalized EL spectra of the WOLEDs E–H at the current density of 10 mA/cm$^2$.

**Table 1**
Performances of the devices A–D.

| | Maximum efficiency (cd/A) | Luminance (cd/m$^2$) at 10 mA/cm$^2$ | CIE coordinates at 1000 cd/m$^2$ |
|---|---|---|---|
| **Device A** | **1.77** | **150** | **(0.154, 0.130)** |
| **Device B** | **3.01** | **280** | **(0.153, 0.143)** |
| **Device C** | **3.06** | **290** | **(0.153, 0.146)** |
| **Device D** | **3.02** | **285** | **(0.153, 0.142)** |

**Table 2**
Performances of the devices E–H.

| | Maximum power efficiency (lm/W) | Maximum luminance (cd/m$^2$) | CIE coordinates at 1000 cd/m$^2$ |
|---|---|---|---|
| **Device E** | **8.2** | **16,490** | **(0.421, 0.460)** |
| **Device F** | **10.7** | **30,120** | **(0.394, 0.430)** |
| **Device G** | **14.8** | **40,870** | **(0.383, 0.418)** |
| **Device H** | **12.3** | **48,900** | **(0.385, 0.422)** |

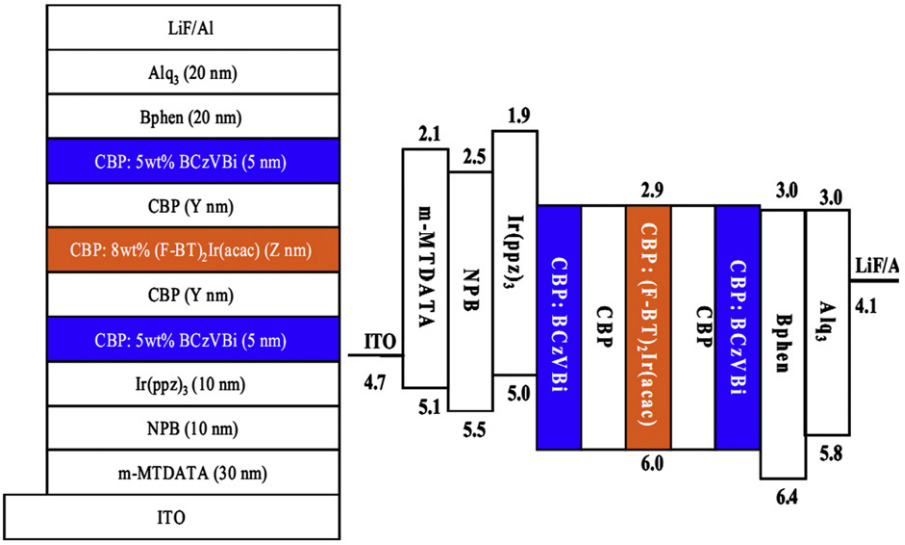


**Fig. 3.** Structure and the energy level diagram of WOLEDs.

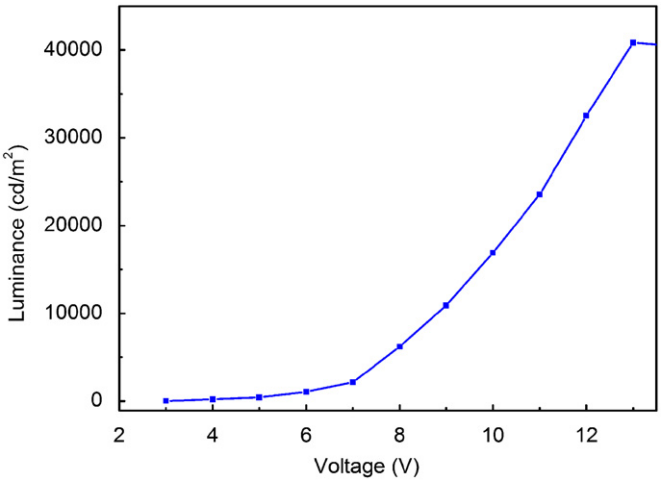


**Fig. 5.** Luminance versus applied voltage of white device G.

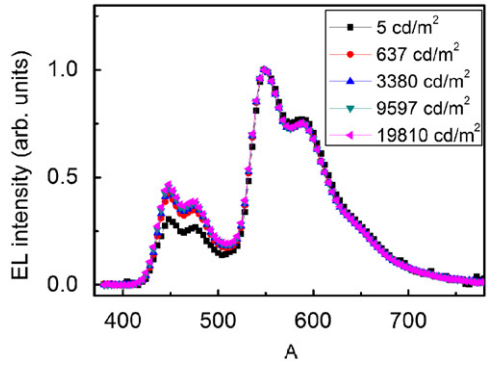


**Fig. 6.** Normalized EL spectra of the white device G at different luminance.

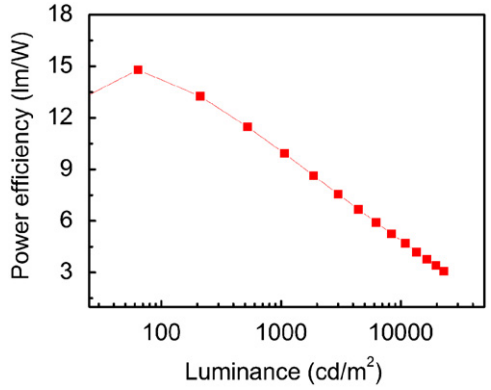


**Fig. 7.** Power efficiency–luminance characteristics of the white device G.

## 4. Conclusion

In summary, we have demonstrated efficient WOLEDs based on blue fluorescence and orange phosphorescence. By exactly adjusting the thickness of emission layers, singlet and triplet excitons are sufficiently utilized by fluorescent and phosphorescent materials, respectively. One white device with a maximum efficiency of 14.8 lm/W has very stable spectra.

## Acknowledgments

This work was supported by Ministry of Science and Technology of China (Grant no. 2010CB327701), National High Technology Research and Development Program of China (Grant no. 2011AA03A110), the National natural science foundation of China (Grant no. 60907013, 60977024, 60706018, 60906021), Science Foundation for Youth of Jilin Province (Grant no. 20090136).

## References

[1] M.A. Baldo, M.E. Thompson, S.R. Forrest, Nature (London) 403 (2000) 750.
[2] B.W. D'Andrade, S.R. Forrest, Adv. Mater. 16 (2004) 1585.
[3] Y. Sun, N.C. Giebink, H. Kanno, B. Ma, M.E. Thompson, S.R. Forrest, Nature (London) 440 (2006) 908.
[4] S.J. Su, E. Gonmori, H. Sasabe, J. Kido, Adv. Mater. 20 (2008) 4189.
[5] S. Reineke, F. Lindner, G. Schwartz, N. Seidler, K. Walzer, B. Lüssem, K. Leo, Nature (London) (2009) 4591038.
[6] M.A. Baldo, M.E. Thompson, S.R. Forrest, Nature (London) 403 (2000) 750.
[7] Y. Duan, M. Mazzeo, V. Maiorano, F. Mariano, D. Qin, R. Cingolani, G. Gigli, Appl. Phys. Lett. 92 (2008) 113304.
[8] G. Schwartz, M. Pfeiffer, S. Reineke, K. Walzer, K. Leo, Adv. Mater. 19 (2007) 3672.
[9] G. Schwartz, S. Reineke, T.C. Rosenow, K. Walzer, K. Leo, Adv. Funct. Mater. 19 (2009) 1.
[10] G. Schwartz, S. Reineke, K. Walzer, K. Leo, Appl. Phys. Lett. 92 (2008) 053311.
[11] P. Anzenbacher. Jr., V.A. Montes, S.Y. Takizawa, Appl. Phys. Lett. 93 (2008) 163302.
[12] G. Schwartz, K. Fehse, M. Pfeiffer, K. Walzer, K. Leo, Appl. Phys. Lett. 89 (2006) 083509.
[13] P.I. Shih, C.F. Shu, Y.L. Tung, Y. Chi, Appl. Phys. Lett. 88 (2006) 251110.
[14] D. Qin, Y. Tao, Appl. Phys. Lett. 86 (2005) 113507.
[15] H. Kanno, R.J. Holmes, Y.R. Sun, S.K. Cohen, S.R. Forrest, Adv. Mater. (Weinheim, Germany) 18 (2006) 339.
[16] B.W. D'Andrade, J. Brooks, V. Adamovich, M.E. Thompson, S.R. Forrest, Adv. Mater. (Weinheim, Germany) 14 (2002) 1032.
[17] G. Cheng, Y.F. Zhang, Y. Zhao, S.Y. Liu, Y.G. Ma, Appl. Phys. Lett. 88 (2006) 083502.
[18] P. Chen, W. Xie, J. Li, T. Guan, Y. Duan, Y. Zhao, S. Liu, C. Ma, L. Zhang, B. Li, Appl. Phys. Lett. 91 (2007) 023505.
[19] U.S. Bhansali, H. Jia, M.A.Q. Lopez, B.E. Gnade, W. Chen, M.A. Omary, Appl. Phys. Lett. 94 (2009) 203501.
[20] L. Zhang, P. Chen, B. Li, Z. Hong, S. Liu, J. Phys. D: Appl. Phys. 41 (2009) 245101.
[21] V. Cleave, G. Yahioglu, P.L. Barny, D.H. Hwang, A.B. Holmes, R.H. Friend, N. Tessler, Adv. Mater. 13 (2001) 44.
[22] M. Cocchi, J. Kalinowski, L. Murphy, J.A.G. Williams, V. Fattori, Org. Electron. 11 (2010) 388.